Diese Arbeit wurde vorgelegt am
Lehr- und Forschungsgebiet Theorie der hybriden Systeme

Optimale Klimakontrolle in Gebäuden mittels linearer Programmierung

Optimal Climate Control in Buildings using Linear Programming

Bachelorarbeit
Informatik

Dezember 2020

Vorgelegt von Presented by	Jesse Germann Kastanienweg 31 52074 Aachen Matrikelnummer: 377545 jesse.germann@rwth-aachen.de
Erstprüfer First examiner	Prof. Dr. rer. nat. Erika Ábrahám Lehr- und Forschungsgebiet: Theorie der hybriden Systeme RWTH Aachen University
Zweitprüfer Second examiner	Prof. Dr.-Ing. Dirk Müller Institute for Energy Efficient Buildings and Indoor Climate RWTH Aachen University
Externer Betreuer External supervisor	Dr. rer. nat. Pascal Richter Steinbuch Centre for Computing Karlsruhe Institute of Technology

Eigenständigkeitserklärung

Hiermit versichere ich, dass ich diese Bachelorarbeit selbständig verfasst und keine anderen als die angegebenen Quellen und Hilfsmittel benutzt habe. Die Stellen meiner Arbeit, die dem Wortlaut oder dem Sinn nach anderen Werken entnommen sind, habe ich in jedem Fall unter Angabe der Quelle als Entlehnung kenntlich gemacht. Dasselbe gilt sinngemäß für Tabellen und Abbildungen. Diese Arbeit hat in dieser oder einer ähnlichen Form noch nicht im Rahmen einer anderen Prüfung vorgelegen.

Aachen, im Dezember 2020

Jesse Germann

Contents

1 Introduction **2**
1.1 Related Work . . . 3
1.2 Outline . . . 5

2 Model for thermal load in buildings **5**
2.1 Thermodynamic Zone Model . . . 5
2.2 Economic Energy Model . . . 10

3 Formulation of optimal control problem **10**
3.1 Optimization process . . . 10
3.2 Linearization . . . 12
3.3 Linear Program . . . 15

4 Solver software **16**
4.1 Solver . . . 16
4.2 Python implementation . . . 16

5 Case Study **17**
5.1 Data . . . 17
5.2 Simulation settings . . . 18
5.3 Testing . . . 20

6 Conclusion and Future Work **25**

References **27**

Symbol	Meaning	Unit
A_{he}	Surface area of the heat exchanger	m^2
A_{w}	Surface area of the walls	m^2
C_{he}	Heat capacity of the heat exchanger	$\frac{J}{^\circ C}$
C_{p}	Constant pressure specific heat of air	$\frac{J}{kg \cdot ^\circ C}$
C_{w}	Heat capacity of the side walls	$\frac{J}{^\circ C}$
f_{mix}	Mixed air Volumetric flow rate	$\frac{m^3}{s}$
f_{o}	Fresh air Volumetric flow rate	$\frac{m^3}{s}$
H_{fg}	Enthalpy of water vapor	$\frac{J}{kg}$
h_{c}	Natural convective heat transfer coefficient	$\frac{W}{m^2 \cdot ^\circ C}$
$h_{\mathrm{v}} V^{\frac{2}{3}}$	Forced convective heat transfer coefficient	$\frac{W}{m^2 \cdot ^\circ C}$
h_{o}	Outdoor heat transfer coefficient	$\frac{W}{m^2 \cdot ^\circ C}$
h_{w}	Heat transfer coefficient in the side walls	$\frac{W}{m^2 \cdot ^\circ C}$
h'_{he}	Heat transfer coefficient on the surface of the heat exchanger	
ℓ	Lewis relation	
ρ	Air density	$\frac{kg}{m^3}$
$p(T)$	Saturated vapor pressure at temperature T	Pa
p_{a}	Vapor pressure of water in thermal space	Pa
p_{s}	Vapor pressure near heat exchanger	Pa
p_{mix}	Vapor pressure of water in mixed air	Pa
p_{o}	Outdoor vapor pressure of water	Pa
Q_{he}	Thermal power from the heat exchanger	W
Q_{in}	Heat input provided by the air conditioning system	W
Q_{load}	Cooling load in the room	W
Q_{w}	Thermal power from the wall	W
r	System-to-fresh-air volumetric flow-rate ratio $\frac{f_{\mathrm{mix}}}{f_{\mathrm{o}}}$	
RH_a	Relative air humidity in thermal space	W
RH_o	Relative air humidity outdoor	W
T_{a}	Temperature in thermal space	°C
T_{he}	Temperature in the heat exchanger surface	°C
T_{mix}	Mix Air temperature	°C
T_{mrt}	Radiant air temperature indoor	°C
T_{o}	Outdoor ambient temperature	°C
T_{s}	Supply air from the heat exchanger	°C
T_{w}	Indoor wall temperature	°C
V_{air}	Relative air velocity indoor	$\frac{m}{s}$
V'_{air}	Relative air velocity in the heat exchanger	$\frac{m}{s}$
V_{he}	Effective heat exchanger volume	m^3
V_{s}	Effective thermal space volume	m^3
W_{a}	Humidity mass ratio in thermal space	
W_{mix}	Humidity mass ratio of mixed air	
W_{o}	Outdoor humidity mass ratio	
W_{s}	Humidity mass ratio of the supply air	

1 Introduction

According to the International Energy Agency (IEA), buildings and their construction account for 36% of global final energy use and 39% of energy-related carbon-dioxide. 30 and 28 percentage points of these fractions can be attributed purely to building operation, respectively. In order to meet the climate goals determined in the Paris Agreement, the average energy intensity per square meter of the global buildings sector requires a decrease of 30% by 2030 (compared to 2015) [7]. This discrepancy is illustrated in Figure 1. Our drastic need for reducing buildings' energy consumption becomes particularly obvious when taking into account that the Earth is expected to reach a population of 8.5 billion by then [14].

A major contributor to the overall energy consumption is summarized by the term HVAC - heating, ventilation and air conditioning. In a typical office building, HVAC alone accounts for roughly 40% of the total building energy consumption [11]. Although "smart" solutions to heating in residential homes are rising in popularity, an automated approach to finding optimal HVAC regulation parameters seems most promising in large-scale commercial buildings. Fortunately, HVAC devices in newer buildings can make use of advancements in information and communication technology and thus realize more complex behavior [3]. By considering factors such as outdoor weather, occupancy and building materials, the objective is therefore to reduce the total energy consumption or - perhaps even more importantly - the cost of operation, whilst still providing thermal comfort and acceptable air quality to all occupants. As energy usage in buildings is often charged with varying prices based on the time of use, the thermal flywheel effect allows operators to pre-heat/pre-cool the building to shift the energy demand in favor of lower costs [20].

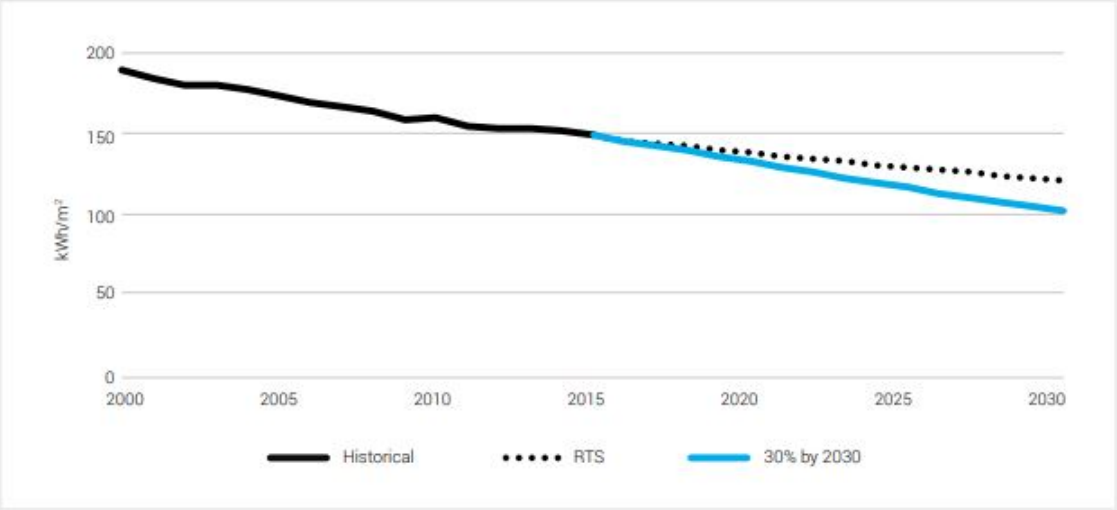

Notes: EJ = exajoules; kWh/m2 = kilowatt-hours per square metre; RTS = Reference Technology Scenario.
Source: IEA (2017), Energy Technology Perspectives 2017, IEA/OECD, Paris www.iea.org/etp/.

Figure 1: Global final energy use per square meter. Historical data is displayed in solid black, whereas the dotted line shows a trajectory under the Reference Technology Scenario, which already takes into account existing energy-related commitments and recent trends. As can be seen, the RTS diverges from the trajectory needed to reach a decrease of 30%, represented by the blue line. [7]

1.1 Related Work

Although on/off and PID controls are still frequently used to control HVAC systems due to their simplicity, many more advanced methods have been developed in recent years [1]. Most of these approaches are based on mathematical models as to move away from corrective control and allow for anticipatory control, handling of constraints and uncertainties and use of advanced optimization algorithms [1]. Researchers have demonstrated that the energy costs associated with HVAC can be greatly reduced by implementing Model Predictive Control (MPC) strategies [8].

Thermodynamic models The ultimate goal in optimal HVAC control is to ensure the thermal comfort of a building's occupants, while minimizing the costs of resources (such as electricity) necessary to achieve this. In order for the controller to predict how a certain HVAC state will affect the building's temperature, a thermodynamic model may be used. Apart from the HVAC system, this model takes into account information such as the weather forecast, building occupation and characteristics of the building. Obviously, the choice of a model is crucial to the accuracy of the resulting predictive control. Heat dynamic models are usually composed of sub models for the mechanisms behind heat transfer [19]. Generally speaking, heat can be transferred through conduction through the walls, through convective air exchange among rooms,

ventilation (e.g. heated air through an open window) and radiation between objects that are in optical contact (e.g. sun exposure) [19, 6, 10]. Often, thermal dynamical models are obtained by modeling the building in question as an RC network [15], which is based on analogies to electrical circuits. Heat transfer and storage are described via circuits of resistances (R) and capacitances (C) [17]. There are many extensive descriptions of such Resistive-Capacitative Models in literature. In [13], a nonlinear model of the overall cooling system (including chillers and storage tanks) has been developed. However, the authors recognize that their model has feasibility issues in real-time implementation.

Zhang et al. [22] present a framework that learns a thermal model for each zone of a building without any manual configuration, given readings from Internet-of-Things-based smart thermostats.

Building performance simulation Building performance simulation (BPS) is a computer-based methodology that aims to replicate certain characteristics and aspects of building performance on the basis of fundamental physical principles. While the complexity of such models may vary, acquiring data and modelling building stocks is generally time-consuming and error-prone [17]. In 2016, Remmen et al. [17] from the E.ON Energy Research Center published a paper on their open framework that covers functionalities for common tasks such as data enrichment and overall facilitates the process of getting building models up and running. In this context, data enrichment means being able to create fully parameterized building models despite sparse data input. The fact that this framework utilizes RC-combinations to model building and wall elements showcases how closely related thermodynamic models and BPS are.

Optimal Control A variety of different predictive control methods for HVAC have been proposed, albeit many of them focus on specific building layouts or subproblems (e.g. only cooling).

Shi et al. [18] have developed an RC-network-based analytical model for multi-zone HVAC precooling to achieve the minimization of total energy costs and peak load demand. Since this model admits a convex approximation, the associated optimization problem can be solved with an efficient distributed algorithm. Their simulation studies indicate an energy cost reduction of up to 60 %. Contrary to many previous controllers assuming deterministic forecasts, Parisio et al. [16] published one of several stochastics-based MPC (SMPC) schemes to take into account uncertainties in weather conditions and occupancy. Based on an RC-network model for the thermal dynamics and a CO_2 concentration model, the strategy dynamically learns the statistics of the building occupancy and weather conditions in order to build probabilistic constraints on the indoor temperature and CO_2 concentration. In a novel approach by Beltran and Cerpa [2], the occupancy of each zone in the building is instead predicted using a Blended Markov Chain (BMC).

According to Wei et al. [20], developing a building dynamics model that is both accurate and efficient enough for effective runtime HVAC control is often intractable.

Hence, they are among many others to propose a data-driven approach. In their case, the HVAC operation is formulated as a Markov decision process. Through deep reinforcement learning (DRL), their framework learns an effective control strategy during building operation, but is then given detailed building dynamics for offline training and validation. Recently, Ostadijafar and Dubey [15] presented an approximate linearized model that leads to an efficient linear model predictive controller (LMPC). Employing a linearization technique for the typically nonlinear thermodynamic model is one possibility of retrieving a computationally feasible controller applicable in real-time control for a building's HVAC system.

The latter essentially describes the idea this thesis builds on. The main point here is to find a reduced model that allows for efficient calculations of globally ideal HVAC control, but still accurately depicts the effects taking place in the building. In particular, we are interested in making the problem solvable by a linear solver.

1.2 Outline

This thesis proceeds as follows: In Section 2, a model for a building's thermal load, i.e. demand for heat energy, is formulated. Based on approximations of this thermal model, the global optimization problem for the HVAC system is then constructed as a linear program in Section 3. Section 4 quickly deals with software employed to compute a solution to this problem. In Section 5, we will then evaluate how well our technique fares with regards to energy and computational efficiency when applied to actual buildings with existing data. The last section concludes our results and provides a short outlook.

2 Model for thermal load in buildings

Since we are taking a physics-based approach, we first need to identify a model that lets us predict how changes in the building's HVAC control will affect its climate under the given conditions. In particular, we would like for the model to take into consideration at least some specific building data (e.g. available heating equiment, construction materials used) and occupancy per thermal zone, as well as a prediction of outdoor weather. Figure 2 illustrates the operating principle of such a thermal model. Note that not every specific model considers all of the listed input parameters, as sometimes accurate predictions on the future indoor climate may be possible without their consideration.

2.1 Thermodynamic Zone Model

Liang and Du [12] provide a thermal space model that is suitable for comfort control and indoor air quality control in a Variable-Air-Volume (VAV) HVAC system. The structure of said model can be seen in Figure 3. The modelled system consists of

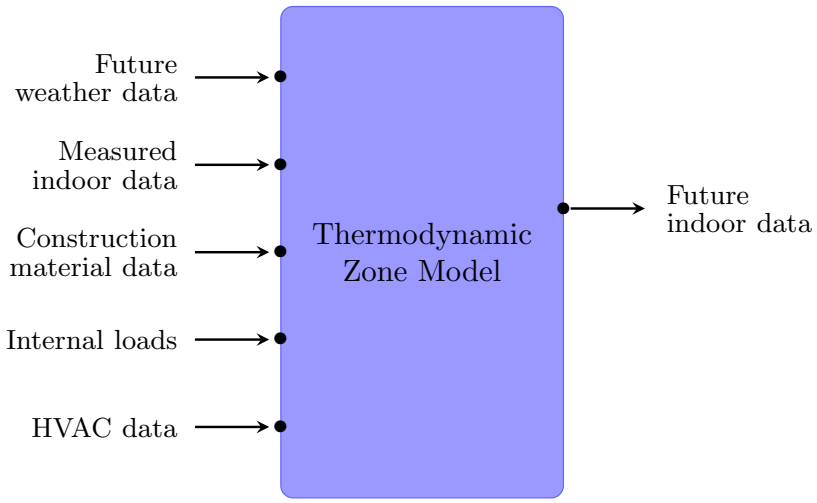

Figure 2: Principle of a thermodynamic zone model - the input consists of future weather data, measured indoor data, construction material data, internal loads, and HVAC data. The output is the resulting future indoor data, which can then be used for the optimization task. Figure slightly altered from [21].

a variable-frequency compressor, a heat exchanger, a variable speed fan, connecting ductwork damper and mix air components.

The following assumptions are made:

1. The wall temperature is equal to the mean radiant temperature: $T_{\mathrm{w}} = T_{\mathrm{mrt}}$
2. The indoor air relative velocity is proportional to the supply air flow rate: $V_{\mathrm{air}} = k \cdot f_{\mathrm{mix}}$
3. The humidity mass ratio W_{a} is proportional to the vapor pressure: $W_{\mathrm{a}} = K_{wv} \cdot p$
4. The heat transfer coefficients h are the sum of a natural convective heat transfer coefficient and a forced convective heat transfer coefficient: $h = h_{\mathrm{c}} + h_{\mathrm{v}} V^{\frac{2}{3}}$
5. Time delay is negligible.

The mathematical model is then derived from the *energy conservation* and *mass balance* in different system components under consideration of both sensible and latent heat exchange. Due to their complexity, the following equations and their derivation may be only partially explained. All symbols used are explained in the nomenclature.

Airflow Mixer The return air and the fresh air are mixed perfectly:

$$T_{\mathrm{mix}} = \frac{1}{r} T_{\mathrm{o}} + \frac{r-1}{r} T_{\mathrm{a}} \tag{1}$$

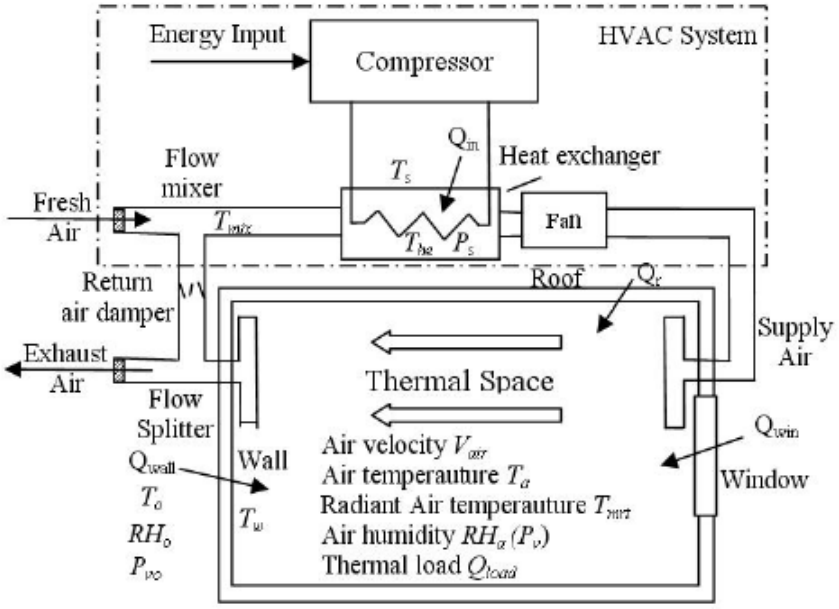

Figure 3: HVAC and Thermal Space Model by Liang and Du [12]

where T_{o} is the outdoor ambient temperature, T_{a} is the temperature in the thermal space and r is the system-to-fresh-air volumetric flow-rate ratio.

$$W_{\mathrm{mix}} = \frac{1}{r} W_{\mathrm{o}} + \frac{r-1}{r} W_{\mathrm{a}} \Rightarrow p_{\mathrm{mix}} = \frac{1}{r} p_{\mathrm{o}} + \frac{r-1}{r} p_{\mathrm{a}} \tag{2}$$

where W_{mix} is the humidity mass ratio of mixed air, W_{o} is the outdoor humidity mass ratio, W_{a} is the humidity mass ratio in the thermal space, p_{mix} is the vapor pressure of water in mixed air, p_{o} is the outdoor vapor pressure of water and p_{a} is the vapor pressure of water in the thermal space.

Heat exchanger for supply air The equations in the heat exchanger are given as balance law:

$$\rho C_{\mathrm{p}} V_{\mathrm{he}} \dot{T}_{\mathrm{s}} = f_{\mathrm{mix}} \rho C_{\mathrm{p}} (T_{\mathrm{mix}} - T_{\mathrm{s}}) + f_{\mathrm{mix}} \rho H_{\mathrm{fg}} K_{\mathrm{wv}} (p_{\mathrm{mix}} - p_{\mathrm{s}}) + Q_{\mathrm{he}} + \ell h'_{\mathrm{he}} \min \left[p(T_{\mathrm{he}}) - p_{\mathrm{s}}, 0 \right] \tag{3}$$

$$K_{\mathrm{wv}} \dot{p}_{\mathrm{s}} = \frac{\ell h'_{\mathrm{he}}}{H_{\mathrm{fg}} V_{\mathrm{he}}} \min \left[p(T_{\mathrm{he}}) - p_{\mathrm{s}}, 0 \right] + K_{\mathrm{wv}} \frac{f_{\mathrm{mix}}}{V_{\mathrm{he}}} (p_{\mathrm{mix}} - p_{\mathrm{s}}) \tag{4}$$

where ρ is the air density, C_{p} is the constant pressure specific heat of air, V_{he} is the effective heat exchanger volume, T_{s} is the supply air from the heat exchanger, f_{mix} is the mixed air volumetric flow rate, T_{s} is the supply air from the heat exchanger, H_{fg} is the enthalpy of water vapor, p_{s} is the vapor pressure near the heat exchanger, Q_{he} is the thermal power from the heat exchanger, ℓ is the Lewis relation, h'_{he} is the heat transfer coefficient on the surface of the heat exchanger and ℓ, h'_{he} and Q_{he} are derived as follows:

$$\ell = \frac{H_{\mathrm{fg}} K_{\mathrm{wv}}}{C_{\mathrm{p}}} \tag{5}$$

$$h'_{\mathrm{he}} = h_{\mathrm{he}} V'^{\frac{2}{3}}_{\mathrm{air}} A_{\mathrm{he}} \tag{6}$$

$$Q_{\mathrm{he}} = h_{\mathrm{he}} V'^{\frac{2}{3}}_{\mathrm{air}} A_{\mathrm{he}} (T_{\mathrm{he}} - T_{\mathrm{s}}) \tag{7}$$

The heat exchanger's governing equation is derived as:

$$C_{\mathrm{he}} \dot{T_{\mathrm{he}}} = -h_{\mathrm{he}} V'^{\frac{2}{3}}_{\mathrm{air}} A_{\mathrm{he}} (T_{\mathrm{he}} - T_{\mathrm{s}}) - \ell h'_{\mathrm{he}} \min \Big[p(T_{\mathrm{he}}) - p_{\mathrm{s}}, 0 \Big] + Q_{\mathrm{in}} \tag{8}$$

Thermal Space The governing equations in the thermal space are given as:

$$\dot{W_{\mathrm{a}}} = \frac{f_{\mathrm{mix}}}{V_{\mathrm{a}}} (W_{\mathrm{s}} - W_{\mathrm{a}}) \Rightarrow \dot{p_{\mathrm{a}}} = \frac{f_{\mathrm{mix}}}{V_{\mathrm{a}}} (p_{\mathrm{s}} - p_{\mathrm{a}}) \tag{9}$$

$$\dot{p_{\mathrm{a}}} = \frac{f_{\mathrm{mix}}}{V_{\mathrm{a}}} (p_{\mathrm{s}} - p_{\mathrm{a}}) \tag{10}$$

$$\rho C_{\mathrm{p}} V_{\mathrm{a}} \dot{T_{\mathrm{a}}} = f_{\mathrm{mix}} \rho C_{\mathrm{p}} (T_{\mathrm{s}} - T_{\mathrm{a}}) + \rho f_{\mathrm{mix}} H_{\mathrm{fg}} K_{\mathrm{wv}} (p_{\mathrm{s}} - p_{\mathrm{a}}) + Q_{\mathrm{load}} + Q_{\mathrm{w}} \tag{11}$$

where Q_{w} includes the thermal power from all walls, windows, the floor, the ceiling and is derived as:

$$Q_{\mathrm{w}} = h_{\mathrm{w}} A_{\mathrm{w}} (T_{\mathrm{w}} - T_{\mathrm{a}}) \tag{12}$$

$$h_{\mathrm{w}} = h_{\mathrm{c}} + h_{\mathrm{v}} V'^{\frac{2}{3}}_{\mathrm{air}} \tag{13}$$

Lastly, the heat transfer process in the side walls can be derived as:

$$C_{\mathrm{w}} \dot{T_{\mathrm{w}}} = -h_{\mathrm{w}} A_{\mathrm{w}} (T_{\mathrm{w}} - T_{\mathrm{a}}) - h_{\mathrm{o}} A_{\mathrm{w}} (T_{\mathrm{w}} - T_{\mathrm{o}}) \tag{14}$$

Taking all the above equations into consideration, the following state-space model for the HVAC and thermal space can be derived:

$$\begin{aligned}
\dot{T_{\mathrm{a}}} =& \frac{f_{\mathrm{mix}}}{V_{\mathrm{a}}} (T_{\mathrm{s}} - T_{\mathrm{a}}) + \frac{f_{\mathrm{mix}} H_{\mathrm{fg}} K_{\mathrm{wv}}}{C_{\mathrm{p}} V_{\mathrm{a}}} (p_{\mathrm{s}} - p_{\mathrm{a}}) + \frac{Q_{\mathrm{load}} + (h_{\mathrm{c}} + h_{\mathrm{v}} V'^{\frac{2}{3}}_{\mathrm{air}}) [A_{\mathrm{w}} (T_{\mathrm{w}} - T_{\mathrm{a}})]}{\rho C_{\mathrm{p}} V_{\mathrm{a}}} \\
\dot{T_{\mathrm{s}}} =& \frac{f_{\mathrm{mix}}}{V_{\mathrm{he}}} [(\frac{1}{r} T_{\mathrm{o}} + \frac{r-1}{r} T_{\mathrm{a}}) - T_{\mathrm{s}}] + \frac{f_{\mathrm{mix}} H_{\mathrm{fg}} K_{\mathrm{wv}}}{C_{\mathrm{p}} V_{\mathrm{he}}} [(\frac{1}{r} p_{\mathrm{o}} + \frac{r-1}{r} p_{\mathrm{a}}) - p_{\mathrm{s}}] \\
& + \frac{h_{\mathrm{he}} V'^{\frac{2}{3}}_{\mathrm{air}} A_{\mathrm{he}} [(T_{\mathrm{he}} - T_{\mathrm{s}}) + \ell \min \Big[p(T_{\mathrm{he}}) - p_{\mathrm{s}}, 0 \Big]]}{\rho C_{\mathrm{p}} V_{\mathrm{he}}} \\
\dot{T_{\mathrm{he}}} =& \frac{-h_{\mathrm{he}} V'^{\frac{2}{3}}_{\mathrm{air}} A_{\mathrm{he}}}{C_{\mathrm{he}}} (T_{\mathrm{he}} - T_{\mathrm{s}}) - \frac{\ell h_{\mathrm{he}} V'^{\frac{2}{3}}_{\mathrm{air}} A_{\mathrm{he}}}{C_{\mathrm{he}}} \min \Big[p(T_{\mathrm{he}}) - p_{\mathrm{s}}, 0 \Big] + \frac{Q_{\mathrm{in}}}{C_{\mathrm{he}}}
\end{aligned}$$

$$
\begin{aligned}
\dot{T_{\mathrm{w}}} =& \frac{-(h_{\mathrm{c}} + h_{\mathrm{v}} V_{\mathrm{air}}^{\frac{2}{3}}) A_{\mathrm{w}}}{C_{\mathrm{w}}} (T_{\mathrm{w}} - T_{\mathrm{a}}) - \frac{h_{\mathrm{o}} A_{\mathrm{w}}}{C_{\mathrm{w}}} (T_{\mathrm{w}} - T_{\mathrm{o}}) \\
\dot{p_{\mathrm{a}}} =& \frac{f_{\mathrm{mix}}}{V_{\mathrm{a}}} (p_{\mathrm{s}} - p_{\mathrm{a}}) \\
\dot{p_{\mathrm{s}}} =& \frac{\ell h_{\mathrm{he}} V_{\mathrm{air}}'^{\frac{2}{3}} A_{\mathrm{he}}}{H_{\mathrm{fg}} V_{\mathrm{he}} K_{\mathrm{wv}}} \min \left[p(T_{\mathrm{he}}) - p_{\mathrm{s}}, 0 \right] + \frac{f_{\mathrm{mix}}}{V_{\mathrm{he}}} [(\frac{1}{r} p_{\mathrm{o}} + \frac{r-1}{r} p_{\mathrm{a}}) - p_{\mathrm{s}}]
\end{aligned}
$$

The variation of indoor cooling / heating load Q_{load}, the ambient temperature T_o and the humidity $RH_o(p_o)$ are taken into consideration in the system design as disturbances. In the given HVAC setup, the three **controllable inputs** provided to the system are:

- Q_{in}: heating/cooling capacity, controlled by the variable-frequency compressor
- f_{mix}: indoor air flow rate, adjusted by the variable-speed fan
- r: system-to-fresh-air volumetric flow-rate ratio, controlled by return air damper

When the system works in heating mode, there will be no water vapor condensation in the heat exchanger. This means we can assume the corresponding term

$$
\min \left[p(T_{\mathrm{he}}) - p_{\mathrm{s}}, 0 \right]
$$

to always be zero. Moreover, if the control parameters f_{mix} and r are adjusted only at certain discrete points in time, they can be treated as constant within each running interval. These two observations lead to the following simplified and linearized model:

$$
\begin{aligned}
\dot{T_{\mathrm{a}}} =& (\frac{f_{\mathrm{mix}}}{V_{\mathrm{a}}}) \cdot T_{\mathrm{s}} + (-\frac{f_{\mathrm{mix}}}{V_{\mathrm{a}}} - \frac{(h_{\mathrm{c}} + h_{\mathrm{v}} V_{\mathrm{air}}^{\frac{2}{3}}) A_{\mathrm{w}}}{\rho C_{\mathrm{p}} V_{\mathrm{a}}}) \cdot T_{\mathrm{a}} + (\frac{(h_{\mathrm{c}} + h_{\mathrm{v}} V_{\mathrm{air}}^{\frac{2}{3}}) A_{\mathrm{w}}}{\rho C_{\mathrm{p}} V_{\mathrm{a}}}) \cdot T_{\mathrm{w}} \qquad (15a) \\
& + (\frac{f_{\mathrm{mix}} H_{\mathrm{fg}} K_{\mathrm{wv}}}{C_{\mathrm{p}} V_{\mathrm{a}}}) \cdot P_{\mathrm{s}} + (-\frac{f_{\mathrm{mix}} H_{\mathrm{fg}} K_{\mathrm{wv}}}{C_{\mathrm{p}} V_{\mathrm{a}}}) \cdot P_{\mathrm{a}} + (\frac{1}{\rho C_{\mathrm{p}} V_{\mathrm{a}}}) \cdot Q_{\mathrm{load}} \\
\dot{T_{\mathrm{s}}} =& (-\frac{f_{\mathrm{mix}}}{V_{\mathrm{he}}} - \frac{h_{\mathrm{he}} V_{\mathrm{air}}'^{\frac{2}{3}} A_{\mathrm{he}}}{\rho C_{\mathrm{p}} V_{\mathrm{he}}}) \cdot T_{\mathrm{s}} + (\frac{(r-1) f_{\mathrm{mix}}}{r V_{\mathrm{he}}}) \cdot T_{\mathrm{a}} + (\frac{h_{\mathrm{he}} V_{\mathrm{air}}'^{\frac{2}{3}} A_{\mathrm{he}}}{\rho C_{\mathrm{p}} V_{\mathrm{he}}}) \cdot T_{\mathrm{he}} \qquad (15b) \\
& + (-\frac{f_{\mathrm{mix}} H_{\mathrm{fg}} K_{\mathrm{wv}}}{C_{\mathrm{p}} V_{\mathrm{he}}}) \cdot P_{\mathrm{s}} + (\frac{(r-1) f_{\mathrm{mix}} H_{\mathrm{fg}} K_{\mathrm{wv}}}{r C_{\mathrm{p}} V_{\mathrm{he}}}) \cdot P_{\mathrm{a}} + (\frac{f_{\mathrm{mix}}}{r V_{\mathrm{he}}}) \cdot T_{\mathrm{o}} + (\frac{f_{\mathrm{mix}} H_{\mathrm{fg}} K_{\mathrm{wv}}}{r C_{\mathrm{p}} V_{\mathrm{he}}}) \cdot P_{\mathrm{o}} \\
\dot{T_{\mathrm{he}}} =& (\frac{h_{\mathrm{he}} V_{\mathrm{air}}'^{\frac{2}{3}} A_{\mathrm{he}}}{C_{\mathrm{he}}}) \cdot T_{\mathrm{s}} + (-\frac{h_{\mathrm{he}} V_{\mathrm{air}}'^{\frac{2}{3}} A_{\mathrm{he}}}{C_{\mathrm{he}}}) \cdot T_{\mathrm{he}} + (\frac{1}{C_{\mathrm{he}}}) \cdot Q_{\mathrm{in}} \qquad (15c) \\
\dot{T_{\mathrm{w}}} =& (\frac{(h_{\mathrm{c}} + h_{\mathrm{v}} V_{\mathrm{air}}^{\frac{2}{3}}) A_{\mathrm{w}}}{C_{\mathrm{w}}}) \cdot T_{\mathrm{a}} + (-\frac{(h_{\mathrm{c}} + h_{\mathrm{v}} V_{\mathrm{air}}^{\frac{2}{3}}) A_{\mathrm{w}}}{C_{\mathrm{w}}} - \frac{h_{\mathrm{o}} A_{\mathrm{w}}}{C_{\mathrm{w}}}) \cdot T_{\mathrm{w}} + (\frac{h_{\mathrm{o}} A_{\mathrm{w}}}{C_{\mathrm{w}}}) \cdot T_{\mathrm{o}} \qquad (15d) \\
\dot{p_{\mathrm{a}}} =& (\frac{f_{\mathrm{mix}}}{V_{\mathrm{a}}}) \cdot P_{\mathrm{s}} + (-\frac{f_{\mathrm{mix}}}{V_{\mathrm{a}}}) \cdot P_{\mathrm{a}} \qquad (15e)
\end{aligned}
$$

$$\dot{p_{\mathrm{s}}} = (-\frac{f_{\mathrm{mix}}}{V_{\mathrm{he}}}) \cdot P_{\mathrm{s}} + (\frac{(r-1)f_{\mathrm{mix}}}{rV_{\mathrm{he}}}) \cdot P_{\mathrm{a}} + (\frac{f_{\mathrm{mix}}}{rV_{\mathrm{he}}}) \cdot P_{\mathrm{o}} \tag{15f}$$

$$\tag{15g}$$

2.2 Economic Energy Model

Since electricity prices depend on the consumer demand for energy, rates can heavily vary from day to day and even by hour. Naturally, we have to take these fluctuations into consideration when modeling an optimal control problem in regards to minimal running cost. For every vector of future control parameters in our HVAC system that leads to an indoor temperature in accordance with the boundaries of the respective timeslot, an economic model estimates the total cost needed to realize this behavior. Figure 4 shows how this model is constructed. The calculations are based on an energy profile that we assume to be known beforehand. The actual optimization routine then uses this information to pick a heating configuration with minimal cost.

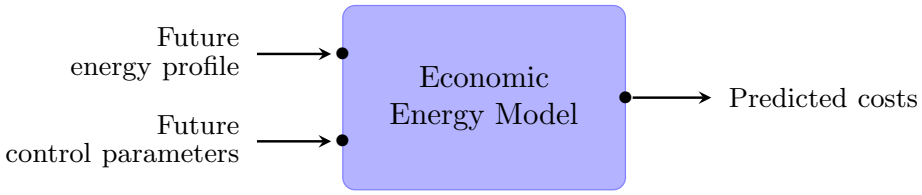

Figure 4: The energy model uses the given energy profile to calculate the predicted total costs of any viable configuration of the control parameters.

3 Formulation of optimal control problem

The thermodynamic model makes it possible to estimate the effect of a specific heating configuration on the system's climate - most importantly the temperature in the thermal space. This estimate can now be used to check whether or not future HVAC control data would lead to an indoor temperature in compliance with the desired boundaries. Since there will usually be many such control inputs, an optimizer is necessary to calculate the most cost-efficient configuration based on the economic energy model. The optimizer will, however, only be taking a finite time horizon into consideration.

3.1 Optimization process

The indoor temperature requirements for the next 48 hours are specified by a so-called *climate profile*. This way, building administration can set time-specific upper and lower boundaries. Based on the building schedule, this very precise regulation allows them to e.g. lower the minimum temperature outside of business hours or during periods in which areas of the building are known to be vacant. As the climate profile in Figure 5

illustrates, the temperature may be kept significantly above the lower boundary if this results in lower overall cost.

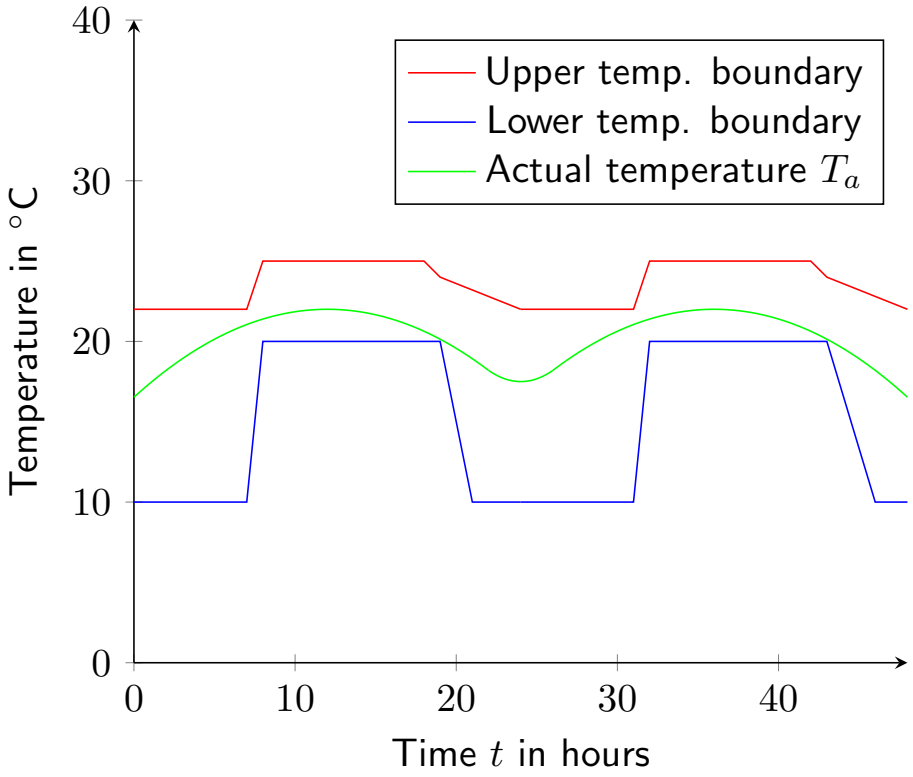

Figure 5: An exemplary climate profile shows how the indoor temperature must always be within the specified bounds, but can otherwise fluctuate freely.

In order to limit the number of adjustments that have to be made to the HVAC system throughout the day, time is divided into n_{time} equal periods of $\Delta t = 15$ minutes. During one period, the HVAC control parameters cannot be changed. After measuring the input data for the thermal model and computing an optimal solution in regards to the current climate profile, the HVAC system runs on the control data specified by the solution only for the first period. Once 15 minutes are over, the climate profile is then extended by one period, the new thermal data is measured and fed into the optimizer again. This process loops continuously, leading to a total of 192 optimizations in 48 hours.

However, when it comes to smart buildings, the limitations of computation resources have to be kept in mind. For practical reasons, single buildings generally are not equipped to carry out their own calculations, but instead rely on a remote computation center which calculates solutions for many buildings at a time and simply sends HVAC instructions to each building. Therefore, a computationally efficient solution to the building's climate control problem is desirable. In this thesis, linear programming is chosen as an optimization routine to get an approximate solution to the optimal control

problem. Linear programs are well-studied and can be solved efficiently. However, since building thermodynamics are known to be highly non-linear (cf. (15)), this modeling choice potentially comes with heavy drawbacks in terms of modeling power.

Linear programming Linear programming is a technique for the optimization of a linear objective function ("cost function") under linear equality and inequality constraints. For variables $x_1, \ldots, x_n$, a linear program (LP) is said to be in *standard form* if it is of the following form:

$$\begin{aligned} \text{maximize} \quad & c_1 x_1 + \cdots + c_n x_n \\ & a_{11} x_1 + \cdots + a_{1n} x_n = b_1 \\ & \vdots \\ \text{subject to} \quad & a_{m1} x_1 + \cdots + a_{mn} x_n = b_m \\ & x_1 \geq 0, \ldots, x_n \geq 0 \end{aligned}$$

Minimization problems with a linear objective function, problems with linear inequality constraints and problems with unbounded or negative variables can easily be transformed into the standard form. Generally, linear programs are solved using basis exchange algorithms (such as the popular simplex algorithm) or using interior-point methods. The simplex algorithm has been proven to solve "random" problems in a cubic number of steps if certain precautions against cycling are taken [4]. Although both solution methods are considered to be similarly efficient for routine applications, one type of solver may be better suited for specific types of LP problems [9].

3.2 Linearization

As input for the LP, we receive measured values for variables $T_s^0, T_a^0, T_{he}^0, T_w^0, P_s^0, P_a^0$ at time 0. If the building does not allow for measurement of all of these values, further assumptions may be made. From the climate profile, boundaries l_i and u_i for $i \in \{1, \ldots, n_{time}\}$ can be derived and the economic energy model returns the cost $cost_i(f_{mix}, Q_{in}, r)$ for a HVAC configuration at time i .

In our thermodynamic zone model (2.1), T_a stands for the temperature of the thermal space. This variable is exactly what needs to be controlled according to the climate profile. Precisely, for all 192 points i in time considered, the approximation of T_a is constrained to be greater than or equal to the lower bound l_i and less than or equal to the upper bound u_i of the specific point:

$$l_i \leq T_a^i \leq u_i \qquad \forall i \in \{1, \ldots, n_{time}\} \tag{16}$$

Since T_a^i depends on the temperature of the previous point T_a^{i-1}, these constraints will actually be of the form

$$l_i \leq T_a^{i-1} + \Delta T_a^i \leq u_i \qquad \forall i \in \{1, \ldots, n_{time}\} \tag{17}$$

Here, ΔT_a^i is a linear term for the total change of T_a from time $i-1$ to i. In order to estimate ΔT_a^i, the derivative of T_a at point $i-1$ will be multiplied by the time of one period.

$$l_i \leq T_a^{i-1} + \Delta t \cdot \dot{T}_a^{i-1} \leq u_i \qquad \forall i \in \{1, \ldots, n_{time}\} \tag{18}$$

Based on the equation for $\dot{T}_a$ specified in the thermal model, we would get the following constraints for T_a^i, $i \in \{1, \ldots, n_{time}\}$:

$$l_i \leq T_a^i \leq u_i \tag{19}$$

$$\begin{aligned} T_a^i = & T_a^{i-1} + \Delta t \cdot \Big[(\frac{f_{\text{mix}}^i}{V_{\text{a}}}) \cdot T_s^{i-1} + (-\frac{f_{\text{mix}}^i}{V_{\text{a}}} - \frac{(h_{\text{c}} + h_{\text{v}} V_{\text{air}}^{\frac{2}{3}}) A_{\text{w}}}{\rho C_{\text{p}} V_{\text{a}}}) \cdot T_a^{i-1} \\ & + (\frac{(h_{\text{c}} + h_{\text{v}} V_{\text{air}}^{\frac{2}{3}}) A_{\text{w}}}{\rho C_{\text{p}} V_{\text{a}}}) \cdot T_w^{i-1} + (\frac{f_{\text{mix}}^i H_{\text{fg}} K_{\text{wv}}}{C_{\text{p}} V_{\text{a}}}) \cdot P_s^{i-1} + (-\frac{f_{\text{mix}}^i H_{\text{fg}} K_{\text{wv}}}{C_{\text{p}} V_{\text{a}}}) \cdot P_a^{i-1} \\ & + (\frac{1}{\rho C_{\text{p}} V_{\text{a}}}) \cdot Q_{\text{load}} \Big] \end{aligned} \tag{20}$$

This is problematic, since f_{mix}^i is part of the controllable parameters (i.e. should be available as a decision variable for each timeslot), but is being multiplied by system variables such as T_s^{i-1} and P_s^{i-1}, which also depend on the choice of control parameters, meaning they have to be modeled as variables in the LP as well. Consequently, the choice of f_{mix} and the current values $T_{\text{s}}, T_{\text{a}}, P_{\text{s}}, P_{\text{a}}$ cannot both be modeled as LP variables, as this product would lead to non-linear terms. The respective constraints of all other system variables that need to be kept track of (such as $T_{\text{s}}, T_{\text{w}}, T_{\text{he}}$ etc.) have the same problem. Therefore, we reduce the decision variables for HVAC control to only

$$Q_{in}^i \text{ for } i \in \{1, \ldots, n_{time}\}$$

This means that nothing but the heat input for the heating system is changed at each timestep, while f_{mix} and r are kept constant, or at least set according to an arbitrary profile known beforehand. In this setting, we assume constant values $\hat{f}_{mix}$ and $\hat{r}$, which effectively makes the system a Constant-Air-Volume (CAV) system. Modeling the controlled input as Q_{in}, rather than f_{mix}, seems reasonable, because the energy cost associated with the former is generally much higher than the electric cost that depends on f_{mix} and r.

Furthermore, testing has shown that estimating a period of 15 minutes (900 seconds) by simply multiplying the derivative at one point by 900 is way too much of an oversimplification to have any practical use. As such, we introduce a new factor s that controls at how many points of a 15-minute period we calculate the new derivatives for all system variables $X \in \{T_a, T_s, T_{he}, T_w, P_a, P_s\}$ based on their current values. Thus, we end up with $n_{time} \cdot s$ variables in the linear program for every $X \in \{T_a, T_s, T_{he}, T_w, P_a, P_s\}$. They still follow the same principle though, and are now connected by the equations

$$X^i = X^{i-1} + \frac{\Delta t}{s} \dot{X}^{i-1}$$

Q_{in} is ultimately our decision variable for each period, so we only have to make sure that the value of Q_{in} is the same for all s steps within one period. Since the variables are in the range of $Q_{in}^0, \ldots, Q_{in}^{n_{time}-1}$, this is simply done by accessing $Q_{in}^{\lfloor \frac{i-1}{s} \rfloor}$ instead of Q_{in}^{i-1}. The same goes for the outdoor temperature, outdoor humidity and temperature boundaries (because we have exactly n_{time} values for all of these, but need to stretch them over $s \cdot n_{time}$ steps). This approximation leads to six linear equations, that can then be used as constraints in a linear program:

$$\begin{aligned} T_a^i =& T_a^{i-1} + \Delta t \cdot \Big[(\frac{\hat{f}_{\text{mix}}}{V_{\text{a}}}) \cdot T_s^{i-1} + (-\frac{\hat{f}_{\text{mix}}}{V_{\text{a}}} - \frac{(h_{\text{c}} + h_{\text{v}} V_{\text{air}}^{\frac{2}{3}}) A_{\text{w}}}{\rho C_{\text{p}} V_{\text{a}}}) \cdot T_a^{i-1} \\ &+ (\frac{(h_{\text{c}} + h_{\text{v}} V_{\text{air}}^{\frac{2}{3}}) A_{\text{w}}}{\rho C_{\text{p}} V_{\text{a}}}) \cdot T_w^{i-1} + (\frac{\hat{f}_{\text{mix}} H_{\text{fg}} K_{\text{wv}}}{C_{\text{p}} V_{\text{a}}}) \cdot P_s^{i-1} + (-\frac{\hat{f}_{\text{mix}} H_{\text{fg}} K_{\text{wv}}}{C_{\text{p}} V_{\text{a}}}) \cdot P_a^{i-1} \\ &+ (\frac{1}{\rho C_{\text{p}} V_{\text{a}}}) \cdot Q_{\text{load}}^{\lfloor \frac{i-1}{s} \rfloor} \Big] \end{aligned} \tag{21a}$$

$$\begin{aligned} T_s^i =& T_s^{i-1} + \Delta t \cdot \Big[(-\frac{\hat{f}_{\text{mix}}}{V_{\text{he}}} - \frac{h_{\text{he}} V_{\text{air}}'^{\frac{2}{3}} A_{\text{he}}}{\rho C_{\text{p}} V_{\text{he}}}) \cdot T_s^{i-1} + (\frac{(\hat{r}-1)\hat{f}_{\text{mix}}}{\hat{r} V_{\text{he}}}) \cdot T_a^{i-1} \\ &+ (\frac{h_{\text{he}} V_{\text{air}}'^{\frac{2}{3}} A_{\text{he}}}{\rho C_{\text{p}} V_{\text{he}}}) \cdot T_{he}^{i-1} + (-\frac{\hat{f}_{\text{mix}} H_{\text{fg}} K_{\text{wv}}}{C_{\text{p}} V_{\text{he}}}) \cdot P_s^{i-1} + (\frac{(\hat{r}-1)\hat{f}_{\text{mix}} H_{\text{fg}} K_{\text{wv}}}{\hat{r} C_{\text{p}} V_{\text{he}}}) \cdot P_a^{i-1} \\ &+ (\frac{\hat{f}_{\text{mix}}}{\hat{r} V_{\text{he}}}) \cdot T_{\text{o}}^{\lfloor \frac{i-1}{s} \rfloor} + (\frac{\hat{f}_{\text{mix}} H_{\text{fg}} K_{\text{wv}}}{\hat{r} C_{\text{p}} V_{\text{he}}}) \cdot P_{\text{o}}^{\lfloor \frac{i-1}{s} \rfloor} \Big] \end{aligned} \tag{21b}$$

$$T_{he}^i = T_{he}^{i-1} + \Delta t \cdot \Big[(\frac{h_{\text{he}} V_{\text{air}}'^{\frac{2}{3}} A_{\text{he}}}{C_{\text{he}}}) \cdot T_s^{i-1} + (-\frac{h_{\text{he}} V_{\text{air}}'^{\frac{2}{3}} A_{\text{he}}}{C_{\text{he}}}) \cdot T_{he}^{i-1} + (\frac{1}{C_{\text{he}}}) \cdot Q_{\text{in}}^{\lfloor \frac{i-1}{s} \rfloor} \Big] \tag{21c}$$

$$\begin{aligned} T_w^i =& T_w^{i-1} + \Delta t \cdot \Big[(\frac{(h_{\text{c}} + h_{\text{v}} V_{\text{air}}^{\frac{2}{3}}) A_{\text{w}}}{C_{\text{w}}}) \cdot T_a^{i-1} + (-\frac{(h_{\text{c}} + h_{\text{v}} V_{\text{air}}^{\frac{2}{3}}) A_{\text{w}}}{C_{\text{w}}} - \frac{h_{\text{o}} A_{\text{w}}}{C_{\text{w}}}) \cdot T_w^{i-1} \\ &+ (\frac{h_{\text{o}} A_{\text{w}}}{C_{\text{w}}}) \cdot T_{\text{o}}^{\lfloor \frac{i-1}{s} \rfloor} \Big] \end{aligned} \tag{21d}$$

$$P_a^i = P_a^{i-1} + \Delta t \cdot \Big[(\frac{\hat{f}_{\text{mix}}}{V_{\text{a}}}) \cdot P_s^{i-1} + (-\frac{\hat{f}_{\text{mix}}}{V_{\text{a}}}) \cdot P_a^{i-1} \Big] \tag{21e}$$

$$P_s^i = P_s^{i-1} + \Delta t \cdot \Big[(-\frac{\hat{f}_{\text{mix}}}{V_{\text{he}}}) \cdot P_s^{i-1} + (\frac{(\hat{r}-1)\hat{f}_{\text{mix}}}{\hat{r} V_{\text{he}}}) \cdot P_a^{i-1} + (\frac{\hat{f}_{\text{mix}}}{\hat{r} V_{\text{he}}}) \cdot P_{\text{o}}^{\lfloor \frac{i-1}{s} \rfloor} \Big] \tag{21f}$$

$$\tag{21g}$$

It is worth noting that Q_{in}, the only choice of controlling the HVAC system, only appears in the equation of T_{he}. This means that in this particular model, a chosen Q_{in}^i can at the earliest show an effect on on the thermal space temperature 3 steps later, as it has to first affect T_{he} in one time-step, which contributes to T_s in the next time-step. Finally, T_s is used in the computation of T_a (21a). However, as long as $s \geq 3$ holds,

this does not change the fact that the temperature T_a is expected to be in the required range after one period, i.e. 15 minutes.

Finally, the variables Q_{in}^i need to be limited to the maximum HVAC capacity of the system at all times. We also need to limit the temperature in the heat exchanger T_{he} to some maximum operating temperature T_{he}^{max}, which is usually given by the manufacturer.

3.3 Linear Program

In conclusion, the full linear program then has the following form:

$$\textbf{minimize} \quad \sum_{i=0}^{n_{time}-1} cost_i(\hat{f}_{mix}, \hat{r}, Q_{in}^i)$$

$$\textbf{s.t.} \ \forall \mathbf{i} \in \{\mathbf{1}, \ldots, \mathbf{n_{time}} \cdot \mathbf{s} - \mathbf{1}\}$$

$$\begin{aligned}
T_a^i =& T_a^{i-1} + \Delta t \cdot \Big[(\frac{\hat{f}_{\text{mix}}}{V_{\text{a}}}) \cdot T_s^{i-1} + (-\frac{\hat{f}_{\text{mix}}}{V_{\text{a}}} - \frac{(h_{\text{c}} + h_{\text{v}} V_{\text{air}}^{\frac{2}{3}}) A_{\text{w}}}{\rho C_{\text{p}} V_{\text{a}}}) \cdot T_a^{i-1} \\
&+ (\frac{(h_{\text{c}} + h_{\text{v}} V_{\text{air}}^{\frac{2}{3}}) A_{\text{w}}}{\rho C_{\text{p}} V_{\text{a}}}) \cdot T_w^{i-1} + (\frac{\hat{f}_{\text{mix}} H_{\text{fg}} K_{\text{wv}}}{C_{\text{p}} V_{\text{a}}}) \cdot P_s^{i-1} + (-\frac{\hat{f}_{\text{mix}} H_{\text{fg}} K_{\text{wv}}}{C_{\text{p}} V_{\text{a}}}) \cdot P_a^{i-1} \\
&+ (\frac{1}{\rho C_{\text{p}} V_{\text{a}}}) \cdot Q_{\text{load}}^{\lfloor \frac{i-1}{s} \rfloor} \Big] \\
T_s^i =& T_s^{i-1} + \Delta t \cdot \Big[(-\frac{\hat{f}_{\text{mix}}}{V_{\text{he}}} - \frac{h_{\text{he}} V_{\text{air}}'^{\frac{2}{3}} A_{\text{he}}}{\rho C_{\text{p}} V_{\text{he}}}) \cdot T_s^{i-1} + (\frac{(\hat{r}-1)\hat{f}_{\text{mix}}}{\hat{r} V_{\text{he}}}) \cdot T_a^{i-1} \\
&+ (\frac{h_{\text{he}} V_{\text{air}}'^{\frac{2}{3}} A_{\text{he}}}{\rho C_{\text{p}} V_{\text{he}}}) \cdot T_{he}^{i-1} + (-\frac{\hat{f}_{\text{mix}} H_{\text{fg}} K_{\text{wv}}}{C_{\text{p}} V_{\text{he}}}) \cdot P_s^{i-1} + (\frac{(\hat{r}-1)\hat{f}_{\text{mix}} H_{\text{fg}} K_{\text{wv}}}{\hat{r} C_{\text{p}} V_{\text{he}}}) \cdot P_a^{i-1} \\
&+ (\frac{\hat{f}_{\text{mix}}}{\hat{r} V_{\text{he}}}) \cdot T_{\text{o}}^{\lfloor \frac{i-1}{s} \rfloor} + (\frac{\hat{f}_{\text{mix}} H_{\text{fg}} K_{\text{wv}}}{\hat{r} C_{\text{p}} V_{\text{he}}}) \cdot P_{\text{o}}^{\lfloor \frac{i-1}{s} \rfloor} \Big] \\
T_{he}^i =& T_{he}^{i-1} + \Delta t \cdot \Big[(\frac{h_{\text{he}} V_{\text{air}}'^{\frac{2}{3}} A_{\text{he}}}{C_{\text{he}}}) \cdot T_s^{i-1} + (-\frac{h_{\text{he}} V_{\text{air}}'^{\frac{2}{3}} A_{\text{he}}}{C_{\text{he}}}) \cdot T_{he}^{i-1} + (\frac{1}{C_{\text{he}}}) \cdot Q_{\text{in}}^{\lfloor \frac{i-1}{s} \rfloor} \Big] \\
T_w^i =& T_w^{i-1} + \Delta t \cdot \Big[(\frac{(h_{\text{c}} + h_{\text{v}} V_{\text{air}}^{\frac{2}{3}}) A_{\text{w}}}{C_{\text{w}}}) \cdot T_a^{i-1} + (-\frac{(h_{\text{c}} + h_{\text{v}} V_{\text{air}}^{\frac{2}{3}}) A_{\text{w}}}{C_{\text{w}}} - \frac{h_{\text{o}} A_{\text{w}}}{C_{\text{w}}}) \cdot T_w^{i-1} \\
&+ (\frac{h_{\text{o}} A_{\text{w}}}{C_{\text{w}}}) \cdot T_{\text{o}}^{\lfloor \frac{i-1}{s} \rfloor} \Big] \\
P_a^i =& P_a^{i-1} + \Delta t \cdot \Big[(\frac{\hat{f}_{\text{mix}}}{V_{\text{a}}}) \cdot P_s^{i-1} + (-\frac{\hat{f}_{\text{mix}}}{V_{\text{a}}}) \cdot P_a^{i-1} \Big] \\
P_s^i =& P_s^{i-1} + \Delta t \cdot \Big[(-\frac{\hat{f}_{\text{mix}}}{V_{\text{he}}}) \cdot P_s^{i-1} + (\frac{(\hat{r}-1)\hat{f}_{\text{mix}}}{\hat{r} V_{\text{he}}}) \cdot P_a^{i-1} + (\frac{\hat{f}_{\text{mix}}}{\hat{r} V_{\text{he}}}) \cdot P_{\text{o}}^{\lfloor \frac{i-1}{s} \rfloor} \Big] \\
T_{he}^i \leq& T_h^{max} e
\end{aligned}$$

$$\forall \mathbf{i} \in \{\mathbf{0}, \ldots, \mathbf{n_{time}} - \mathbf{1}\}$$
$$0 \leq Q_{in}^{i} \leq Q_{in}^{max}$$
$$\forall \mathbf{i} \in \{\mathbf{s}, \ldots, \mathbf{n_{time}} - \mathbf{1}\}$$
$$l_i \leq T_a^i \leq u_i$$

Since $\hat{f}_{mix}$ and $\hat{r}$ are no longer variables, the cost function in the objective really only depends on $Q_{in}^{i}, i \in \{0, \ldots, n_{time} - 1\}$.

4 Solver software

4.1 Solver

There are a variety of commercial and non-commercial solvers for linear programs available. Since we have no limitation of any variables (e.g. to integers), the solver does not have to be capable of solving mixed-integer programs for this application. The most common solvers appear to include:

- **Gurobi.** As Gurobi is commercial software known for short execution times, it is expected to outperform the alternatives. An academic license makes it usable for this thesis.
- **GLPK.** The GNU Linear Programming Kit is an open-source C library available under the GNU General Public License callable to solve both linear and mixed-integer programming problems.
- **LP_solve.** LP_solve is also written in C and available for download under the `LGPL 2` license. Besides linear programming and mixed-integer programming problems, LP_solve can also be used for semi-continuous and special ordered sets (SOS) problems

Once an LP model has been created using either of these solutions, it can be stored into an `MPS`-file and then easily solved using another solver. Our problem is originally modeled using `Gurobi 8.1.1` for `Python 3.8.5`, as a commercial software like Gurobi is expected to outperform the other ones.

4.2 Python implementation

The structure of the implementation is quite simple, as it consists of just four Python files. The most important components are `lp_mpc.py` and `simulations.py`, while the other two provide minor functionality.

`lp_mpc.py` Provides the LP class and a `solve` method for solving the LP established in Subsection 3.3 based on the necessary input parameters. These include a `Settings` object and an object carrying `PhysicalConstants`.

`simulations.py` Executes the main code for simulating the behavior in an MPC setting. Begins by reading in static data for the settings and constants, as well as dynamic data for the lower/upper boundaries and temperature forecasts from CSV-files. The method `run_n_lps` solves an individual LP for each time-point $i = 1, \ldots, n_runs$ with a time-horizon of n_time datapoints. The results for each LP are then written into a new CSV file.

The packages used (e.g. `pandas`, `numpy`) are all part of the Anaconda Python distribution.

5 Case Study

In the following, simulations are conducted on real-world data to verify the effectiveness of our approach. The data has been provided by MeteoViva. The Jülich-based company works on smart data solutions for commercial real estate and is a leader in intelligent building management.

5.1 Data

The data of one test case is stored as a comma-separated values (CSV) file, where each row describes all the input values at one time-step. Time-steps are 15 minutes apart. For the purposes of this thesis, most of the given values (such as a forecast of the outdoor wind-speed, outdoor radiation) can be disregarded, because the model chosen in 2.1 primarily considers outdoor temperature and humidity ratio as outside factors in its calculations of temperature changes. Additionally, upper and lower temperature limits for each point in time are given.

The graph in Figure 6 allows us to gain a better understanding of the data provided, as it visualizes the relation between upper limit, lower limit and outdoor temperature. Note how the upper limit stays at a constant $34°C$, while the lower limit oscillates between 18 and $22°C$ based on the night-day-cycle. Additionally, the course of the indoor temperature under a given HVAC optimization strategy is displayed in green. Note how it permanently stays above the higher lower limit, $22°C$.

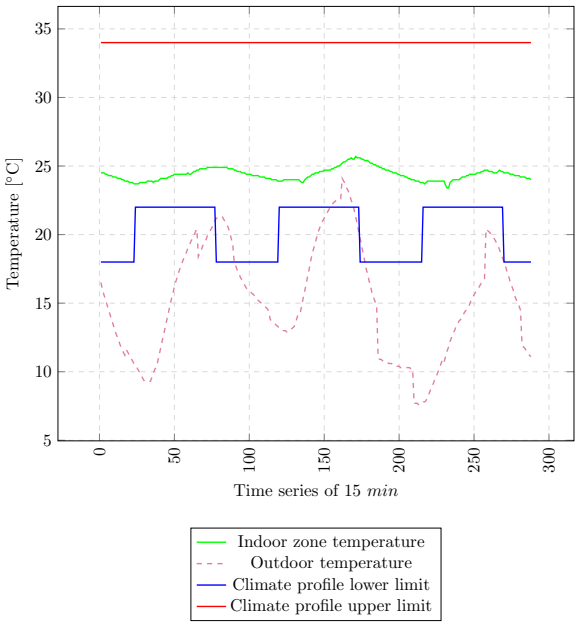

Figure 6: Data visualization for 3 days in April. There is a duration of 15 minutes between two data points.

5.2 Simulation settings

There are a variety of very specific physical values used in the model 15 that serve as the basis of our approach; however, the authors only explicitly state the values for some major simulation parameters [12]. Therefore, the missing constants had to be ”filled in” through research and an attempt to recover values from the computed matrices that Liang and Du provide in the paper. For lack of suitable data, energy prices are assumed to be constant here.

Our simulation deals with the heating of a single zone, namely a room of dimensions 5 by 5 meters and a height of 3 meters. The constant values f_{mix} and r have been chosen to ensure an adequate amount of air-flow in the thermal space. Certain values like the enthalpy of water vapor, which is normally a function of temperature, have been assumed as constant in the given heating setting. The wall heat capacity of 1614688.91 $\frac{J}{°C}$ is the product of the specific heat capacity of the wall material and the wall's total mass. As for the heat exchanger, it has an effective volume of 1 cubic meter, a surface area of 1 square meter and a maximum operational temperature of 90 degrees Celsius. All important parameters are listed in Table 1 below. Note that a few values (such as the natural and forced convective heat transfer coefficient) could not be separated based on the information given; however, they only appear in the computations in conjunction. The maximum HVAC capacity is 12 kWh.

Symbol	Meaning	Unit	Value
f_{mix}	Mixed air volumetric flow-rate	$\frac{m^3}{s}$	0.272
r	System-to-fresh-air volumetric flow-rate ratio	$\frac{f_{\text{mix}}}{f_{\text{o}}}$	4
V_{he}	Effective heat exchanger volume	m^3	1
V_{a}	Volume of thermal space	m^3	75
ρ	Air density	$\frac{kg}{m^3}$	1.19592
C_{p}	Constant pressure specific heat of air	$\frac{J}{kg \cdot ^\circ C}$	1000
C_{he}	Heat capacity of the heat exchanger	$\frac{J}{^\circ C}$	30000
A_{he}	Surface area of the heat exchanger	m^2	1
$h_{he} \cdot V_{\text{air}}'^{\frac{2}{3}}$	Heat exchanger transfer coefficient	$\frac{W}{m^2 \cdot ^\circ C}$	408.6459
$h_{\text{c}} + h_{\text{v}} V_{air}^{\frac{2}{3}}$	Natural and forced convective heat transfer coefficient	$\frac{W}{m^2 \cdot ^\circ C}$	3.3625533
A_{w}	Surface area of the walls, windows etc.	m^2	110
C_{w}	Heat capacity of the side walls	$\frac{J}{^\circ C}$	1624065.26
$K_{\text{wv}} \cdot H_{\text{fg}}$	Enthalpy of water vapor multiplied by factor of $K_{wv} = \frac{W_{\text{a}}}{p}$	$\frac{J}{kg}$	15165.44
Q_{load}	Indoor heat load	W	1600

Table 1: Simulation settings for the (pre-)computation of the state-space model

$$\begin{bmatrix} \dot{T}_s \\ \dot{T}_a \\ \dot{T}_{he} \\ \dot{T}_w \\ \dot{p}_s \\ \dot{p}_a \end{bmatrix} = \begin{bmatrix} -0.6137 & 0.2040 & 0.3417 & 0 & -4.1274 & 3.0955 \\ 0.0036 & -0.0077 & 0 & 0.0041 & 0.0550 & -0.0550 \\ 0.0136 & 0 & -0.0136 & 0 & 0 & 0 \\ 0 & 2.2775\text{e-}004 & 0 & -5.4650\text{e-}004 & 0 & 0 \\ 0 & 0 & 0 & 0 & -0.2720 & 0.2040 \\ 0 & 0 & 0 & 0 & 0.0036 & -0.0036 \end{bmatrix} \begin{bmatrix} T_s \\ T_a \\ T_{he} \\ T_w \\ P_s \\ P_a \end{bmatrix}$$

$$+ \begin{bmatrix} 0.0680 & 1.0318 & 0 \\ 0 & 0 & 1.1149\text{e-}005 \\ 0 & 0 & 0 \\ 3.1875\text{e-}004 & 0 & 0 \\ 0 & 0.0680 & 0 \\ 0 & 0 & 0 \end{bmatrix} \begin{bmatrix} T_o \\ P_o \\ Q_{load} \end{bmatrix} + \begin{bmatrix} 0 \\ 0 \\ 3.3333\text{e-}005 \\ 0 \\ 0 \\ 0 \end{bmatrix} Q_{in}$$

Figure 7: Once all the values have been inserted into the model's equations, the state-space model in matrix form looks like this [12].

When running the optimization LP, we generally initialize T_s, T_a, T_{he}, T_w to the outdoor temperature at that given time. However, our data does not include values for any

water vapor pressure, which are necessary for both the initialization of P_s, P_a and the consideration of outdoor humidity by means of P_o (the water vapor pressure outside). Knowing that the simulation in Du and Liang's paper appears to start at $6°C$ and the initial thermal space humidity and supply air humidity are given as roughly 56% and 43%, we can calculate the respective amounts of water vapor pressure assumed.

The Arden Buck equation [5] for positive temperatures can be applied to calculate the saturation vapor pressure of moist air at the initial temperature.

$$P(t) = 611,21 \cdot exp((18.678 - t/234.5) \cdot (t/(257.14 + t)))$$

For a temperature of $t = 6°C$, the formula returns a saturation pressure of 935.2 Pascal. Therefore, we will initialize P_a^0 as $0.56 \cdot 935.2 = 523.71$ and P_s^0 as $0.43 \cdot 935.2 = 402.14$. When it comes to the outdoor vapor pressure P_o, the original settings of $4 - 12°C$ and relative humidity of 45 to 65 percent mean that 520 Pascal can be considered a suitable value.

5.3 Testing

Frequency of model evaluations (controlled by s) In a first set of tests, the goal was to establish a suitable value for s, meaning the number of discrete evaluation points of the thermal model within each period of 15 minutes. Since s is directly proportional to the number of linear variables that have to be solved, trying to follow the model's continuous progress too closely may easily make the runtime impractically large.
The following diagrams show a comparison of the time needed to find an optimal solution by `Gurobi` against the total energy spent in that solution. A time horizon of 96 points, i.e. 24 hours, was considered. As can be seen in Figure 8, the performance of a solution does not seem to be affected by s, as rounding the results to 2 digits leads to the same energy consumption. A number of executions using different conditions have confirmed this result.

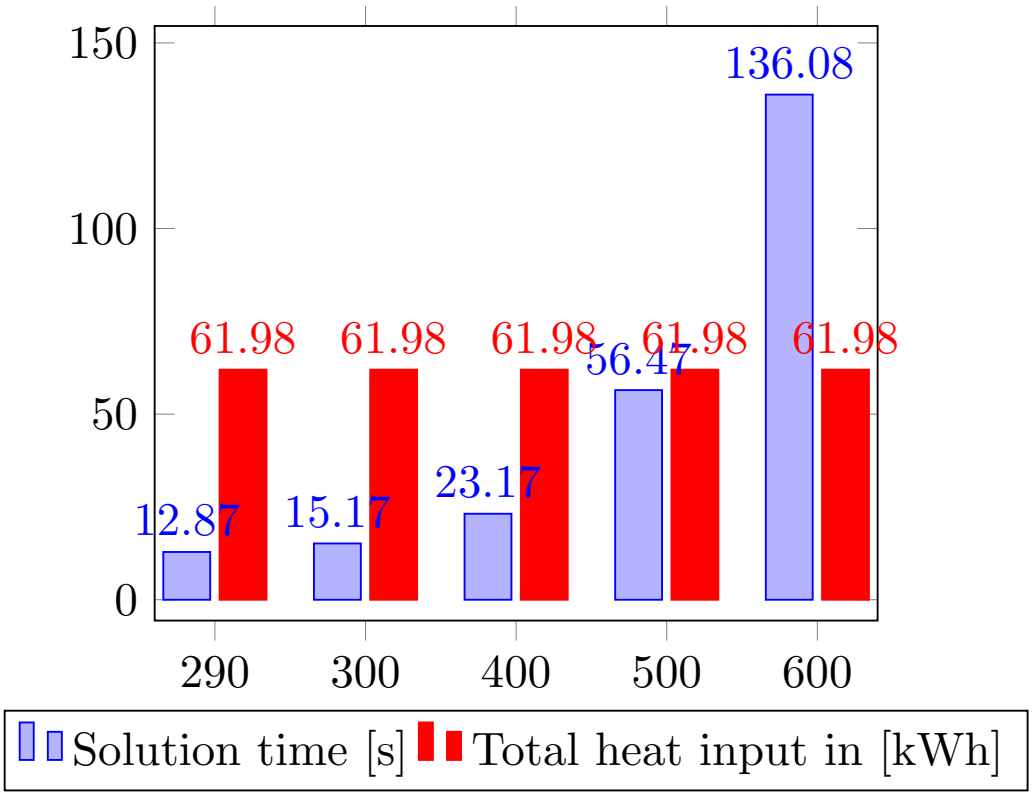

Figure 8: Comparison of results using different values of s and a time horizon of $n_{time} = 96$, i.e. 24 hours

Clearly, s is exponentially related to the solution time. While the runtimes may be acceptable for higher values of s with a time horizon of 24 hours, further tests have shown that this growth becomes even more drastic when considering a time horizon of 48 hours. Therefore, s was set to 300 from this point on, as s had been shown to not affect the quality of the solution significantly.

For values below 290 (e.g. 280), which correspond to timeslots of 3.1 seconds or more, the LP was usually unable to find valid solutions. This is an interesting finding, as the invariance of the total heat input in all optimal solutions could have led one to believe that even smaller values for s would be "accurate enough" to depict the changes of the system. Unfortunately, the run for $s = 290$ did not hint towards any obvious conditions for an LP to be infeasible. The results for $s = 290$ can be seen in Figure 9.

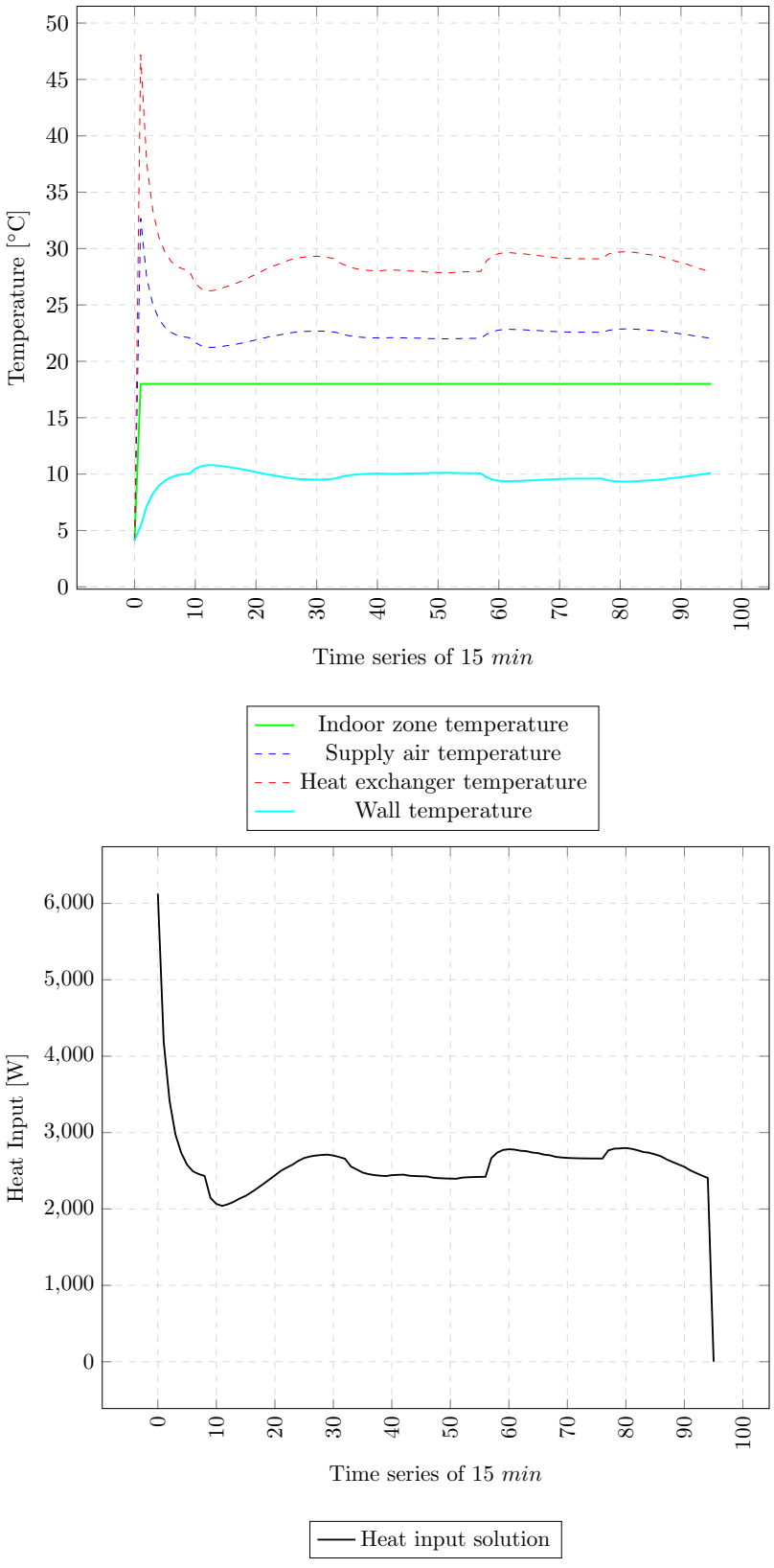

Figure 9: Heating response for $s = 290$, time horizon of 24 hours; Data from January 2, 2019

Time horizon settings One of the main goals of this approach at controlling heating intelligently was to make use of knowledge about the future; namely, the future outdoor temperature and indoor temperature boundaries. Coupled with a thermodynamic model, one idea was that the heating system could possibly save energy by heating more than necessary to reach the lower temperature boundary, and then stop heating to let the energy stored in walls and heat exchanger fuel the indoor temperature for some time. In practice, future data and the ability to plan more "long-term" turned out to not play a significant role.

In a number of tests, the influence of the window size n_{time} on the total heat input over a period of time has been investigated. For this purpose, our model is running in "MPC-mode": after solving the LP with a window size of n_{time}, the resulting system variables (temperatures and vapor pressures) after the first heating period of 15 minutes are stored. For the computation of the next LP, the stored temperatures and vapor pressures are used as initial values. This leads to a simulation of our model's behavior in a real application, if we assume the thermodynamic model as perfectly predicting the resulting system state.

Time horizon considered	Total energy [W]
2	55786.72
4	55777.33
6	55776.37
8	55776.05
10	55776.05
20	55776.04
48	55776.04

Figure 10: Results in MPC mode over a time-span of 12 hours. Increasing the time horizon led to almost no improvement in total energy spent.

The smallest possible window size is 2, which means future data is only available for one time-step. This essentially makes the system greedily decide the bare minimum it has to currently heat in order to meet the temperature requirements 15 minutes later. In contrast to that, a larger window size like 48 should enable the system to make more strategic decisions. For window sizes ranging from 2 to 48, a series of 48 consecutive linear programs was solved (simulating half a day of system behavior). The system performance for a window size of 2 and 48 and their can be seen in Figure 11. Executions with a higher time horizon had only minimally better performance, especially when putting the savings in relation to the absolute energy usage. Evidently, even when able to plan the heating process for a longer period in advance, the optimal solution was always to heat as little as currently possible. This leads to a smooth heating process at somewhat lower input, as opposed to heating at full power for a bit and then turning heating off. Testing under different circumstances (lower/higher outside temperatures, lower temperature limit changing) changed nothing about the

outcome.

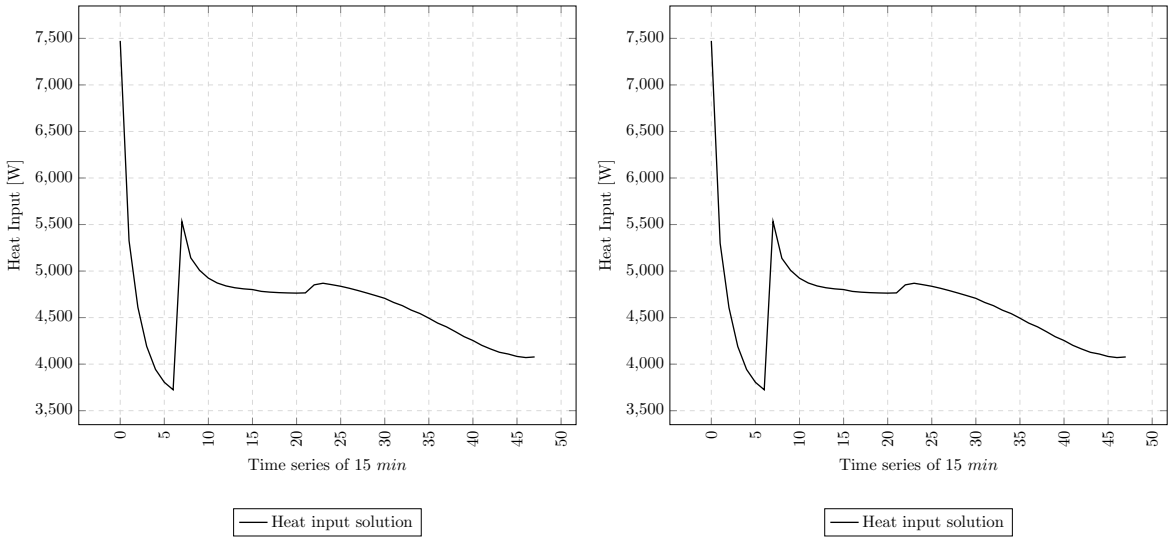

Figure 11: Comparison between heating solutions for time horizon 2 (left) and 48 (right) over a course of 12 hours. Differences are practically unnoticeable.

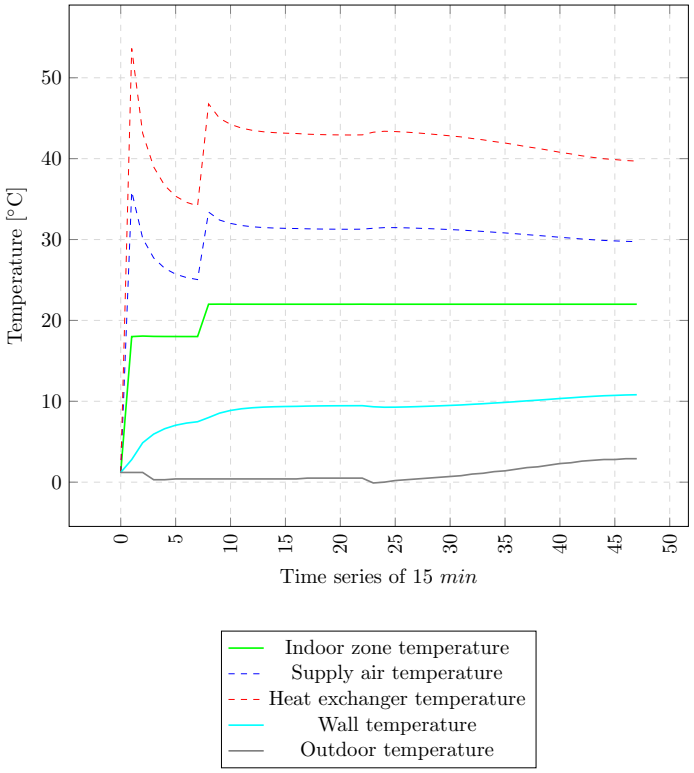

Figure 12: Shared heating response for window sizes 2 and 48.

Other observations Especially during the initial testing phase, the importance of the vapor pressure values quickly became apparent. Notably the values for P_o, which we assumed as a constant of 520 Pascal, had a large impact on the behavior of the system. When tested with a fixed heat input of 0, changing P_o slightly could easily result in unrealistically quick drops in temperature (below the outside temperature). Overall, the importance of vapor pressure values in the thermodynamic zone model may be considered a point of criticism, as these unrealistic cases suggest that the treatment of these pressure values may have fallen victim to oversimplification.

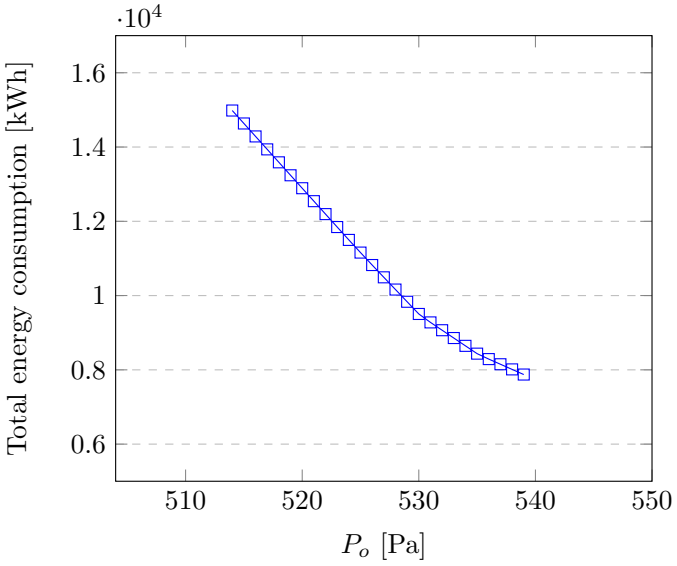

Figure 13: Total energy consumption in a 3-hour-window based on choice of constant outdoor vapor pressure P_o.

Figure 13 shows the total energy consumption for heating under different values for the outdoor vapor pressure P_o. Despite only considering a horizon of 12 points (3 hours) and keeping everything else fixed, an enormous change in energy efficiency can be seen with rising P_o, with consumption dropping from 14634.54 to 7873.82 watt-hours. All values for P_o below 514 and above 540 Pascal created a control problem that was unsolvable.

Generally, the energy used for heating turned out high in comparison to average heating consumption in buildings. Part of the reason for this outcome probably lies in the simulation design: Since the simulation deals with a single room that is only separated from the outside world through one layer of walls, the thermal space is more susceptible to being influenced by cold weather than an average room in a building.

6 Conclusion and Future Work

All in all, the ”predictive” power of this approach turned out to be somewhat limited, as the considered time horizon has been shown to have nearly no impact on the chosen

HVAC settings. Still, our model enables a user to enter precise temperature requirements for exact points in time that will automatically be satisfied under real-time consideration of outdoor temperature and the current indoor state. In general, the approach of computing derivatives at a set number of points and thus approximating the actual system progression is a very interesting idea to me. I was particularly surprised by the fact that dropping s as low as 300 (i.e. 3 seconds per time-step) did not appear to cause any major loss of precision.

Whilst the simulations in this thesis were limited to one thermodynamic zone, it can potentially be adapted for entire large-scale buildings, where T_o instead refers to the temperature in neighboring rooms. Implementing this would certainly require some more considerations than dealt with in this thesis, but based on the rather simple design of the state-space model, it appears well-scalable.

In the future, it would make sense to feed the heating configurations acquired by means of linear programming into a more accurate (but usually slower) simulation system, in order to verify the effectiveness of the chosen heat inputs. Since building dynamics are often described as complex and highly non-linear, it is compelling to see how well a simple control system operating through linear computations can really fare. As for now, no such simulation software was easily obtainable. Perhaps, adapting a model of a heating system more commonly found in Germany would have even made that possible within the scope of this thesis. In the scope of a bigger project, a building performance simulation tool such as TEASER [17] would probably allow me to test exactly this behavior.

Nonetheless, if the already very detailed outside data-set were accompanied by at least relative humidity ratio, which is usually publicly available in real-time, it would give a lot more credibility to the results of our computations.

The fact that researchers such as Ostadijafari et al. [15] tackled the very same problem of creating a linear model-predictive controller for HVAC just last year (2019), shows that there is still a lot of on-going work and opportunity in this particular research field. In future works, their more sophisticated approach of applying feedback linearization techniques to deal with nonlinear thermal building dynamics could be further pursued, as it has shown promising results.

References

[1] Abdul Afram and Farrokh Janabi-Sharifi. Review of modeling methods for hvac systems. *Applied Thermal Engineering*, 67(1-2):507–519, 2014. ISSN 1359-4311. doi: 10.1016/j.applthermaleng.2014.03.055.

[2] Alex Beltran and Alberto E. Cerpa. Optimal hvac building control with occupancy prediction. In *Proceedings of the 1st ACM Conference on Embedded Systems for Energy-Efficient Buildings*, BuildSys '14, page 168–171, New York, NY, USA, 2014. Association for Computing Machinery. ISBN 9781450331449. doi: 10.1145/2674061.2674072. URL `https://doi.org/10.1145/2674061.2674072`.

[3] Gianni Bianchini, Marco Casini, Daniele Pepe, Antonio Vicino, and Giovanni Gino Zanvettor. An integrated model predictive control approach for optimal HVAC and energy storage operation in large-scale buildings. *APPLIED ENERGY*, 240: 327–340, APR 15 2019. ISSN 0306-2619. doi: {10.1016/j.apenergy.2019.01.187}.

[4] Karl Heinz Borgwardt. *The simplex method. A probabilistic analysis*, volume 1. Springer, Berlin, 1987.

[5] Arden L. Buck. New Equations for Computing Vapor Pressure and Enhancement Factor. *Journal of Applied Meteorology*, 20(12):1527–1532, December 1981. doi: 10.1175/1520-0450(1981)020<1527:NEFCVP>2.0.CO;2.

[6] K. Deng, P. Barooah, P. G. Mehta, and S. P. Meyn. Building thermal model reduction via aggregation of states. In *Proceedings of the 2010 American Control Conference*, pages 5118–5123, 2010.

[7] UN Environment and International Energy Agency. Towards a zero-emission, efficient, and resilient buildings and construction sector. global status report 2017. Technical report, 2017.

[8] Hao Huang, Lei Chen, and Eric Hu. A new model predictive control scheme for energy and cost savings in commercial buildings: An airport terminal building case study. *Building and Environment*, 89:203 – 216, 2015. ISSN 0360-1323. doi: https://doi.org/10.1016/j.buildenv.2015.01.037. URL `http://www.sciencedirect.com/science/article/pii/S0360132315000530`.

[9] Tibor Illés and Tamás Terlaky. Pivot versus interior point methods: Pros and cons. *European Journal of Operational Research*, 140(2):170–190, 2002. ISSN 0377-2217. doi: 10.1016/s0377-2217(02)00061-9.

[10] Ciprian Lapusan, Radu Balan, Olimpiu Hancu, and Alin Plesa. Development of a multi-room building thermodynamic model using simscape library. *Energy Procedia*, 85:320 – 328, 2016. ISSN 1876-6102. doi: https://doi.org/10.1016/j.egypro.2015.12.258. URL `http://www.sciencedirect.com/science/article/pii/S1876610215029239`. EENVIRO-YRC 2015 - Bucharest.

[11] Lasath Lecamwasam, John Wilson, and David Chokolich. *Guide to best practice maintenance & operation of HVAC systems for energy efficiency / this document is written by Lasath Lecamwasam, John Wilson and David Chokolich*. Department of Climate Change and Energy Efficiency [Canberra]. ISBN 9781922003157.

[12] Jian Liang and Ruxu Du. *Thermal comfort control based on neural network for HVAC application*. doi: 10.1109/cca.2005.1507230.

[13] Yudong Ma, F. Borrelli, B. Hencey, B. Coffey, S. Bengea, and P. Haves. Model predictive control for the operation of building cooling systems. *IEEE Transactions on Control Systems Technology*, 20(3):796–803, 2012. ISSN 1063-6536. doi: 10.1109/tcst.2011.2124461.

[14] United Nations Department of Economic and Social Affairs. *World Urbanization Prospects 2018: Highlights*. 2019. doi: https://doi.org/https://doi.org/10.18356/6255ead2-en. URL `https://www.un-ilibrary.org/content/publication/6255ead2-en`.

[15] M. Ostadijafari and A. Dubey. Linear model-predictive controller (lmpc) for building's heating ventilation and air conditioning (hvac) system. In *2019 IEEE Conference on Control Technology and Applications (CCTA)*, pages 617–623, 2019.

[16] Alessandra Parisio, Damiano Varagnolo, Daniel Risberg, Giorgio Pattarello, Marco Molinari, and Karl Johansson. Randomized model predictive control for hvac systems. pages 1–8, 11 2013. doi: 10.1145/2528282.2528299.

[17] Peter Remmen, Moritz Lauster, Michael Mans, Marcus Fuchs, Tanja Osterhage, and Dirk Müller. Teaser: an open tool for urban energy modelling of building stocks. *Journal of Building Performance Simulation*, 11(1):84–98, 2018. doi: 10.1080/19401493.2017.1283539. URL `https://doi.org/10.1080/19401493.2017.1283539`.

[18] Hongsen Shi, Jia Liu, and Qian Chen. Hvac precooling optimization for green buildings: An rc-network approach. In *Proceedings of the Ninth International Conference on Future Energy Systems*, e-Energy '18, page 249–260, New York, NY, USA, 2018. Association for Computing Machinery. ISBN 9781450357678. doi: 10.1145/3208903.3208920. URL `https://doi.org/10.1145/3208903.3208920`.

[19] Anders Thavlov and Henrik W. Bindner. Thermal models for intelligent heating of buildings. 2012.

[20] Tianshu Wei, Yanzhi Wang, and Qi Zhu. *Deep Reinforcement Learning for Building HVAC Control*. 2017. doi: 10.1145/3061639.3062224.

[21] K. Yaneva. Optimized control for climate in buildings using artificial intelligence. Bachelor's thesis, RWTH Aachen University, 2019.

[22] Xiangyu Zhang, Manisa Pipattanasomporn, Tao Chen, and Saifur Rahman. An IoT-Based Thermal Model Learning Framework for Smart Buildings. *IEEE INTERNET OF THINGS JOURNAL*, 7(1):518–527, JAN 2020. ISSN 2327-4662. doi: {10.1109/JIOT.2019.2951106}.